Space-Time Weighted Nonbinary Repeat-Accumulate Codes in Frequency-Selective MIMO Channels

Kai Yen*†
* Institute for Infocomm Research
21 Heng Mui Keng Terrace, Singapore 119613
Email: yenkai@i2r.a-star.edu.sg

Nenad Veselinovic† and Tadashi Matsumoto†
† University of Oulu
P.O. Box 4500, FIN-90014 University of Oulu, Finland
Email: {yenkai,nenad,tadashi.matsumoto}@ee.oulu.fi

***Abstract*— The so-called space-time weighted nonbinary repeat-accumulate (ST-WNRA) codes are capable of achieving full antenna diversity in single-user flat fading channels. In this paper, the performance of these codes is evaluated over a frequency-selective Rayleigh fading multiple-input multiple-output channel in a multiuser environment. Under this channel condition, the full antenna diversity supported by the ST-WNRA codes can no longer be achieved due to the presence of intersymbol interference and multiple access interference. Hence, in order to suppress these interferences, a turbo equalization technique based on the minimum mean square-error filtering with soft interference cancellation (SC-MMSE) is employed. The SC-MMSE detector is designed such that the diversity that can be gleaned from the multiple antennas as well as from the multipath components can be fully exploited. Computer simulations demonstrate that our proposed turbo-equalized system with ST-WNRA codes is capable of achieving the maximum diversity order and hence achieving an excellent bit error rate performance with a reasonable spectral efficiency at a low complexity cost.**

I. Introduction

The notion of diversity has been widely accepted as one of the most important component for reliable wireless communications. Information theoretic aspects of transmit diversity studied in [1], [2] have demonstrated that the capacity of multiple-antenna systems significantly exceeds that of single-antenna systems in scattering-rich fading channels. These promising results prompted the development of several so-called space-time coding (STC) schemes [3]–[5]. Recently, Oh and Yang [6] proposed the so-called space-time weighted nonbinary repeat-accumulate (ST-WNRA) codes, which was shown to have a rank equivalent to $\min(r, N_T)$, where N_T is the number of transmit antennas and r is the number of symbol repetitions. Furthermore, ST-WNRA codes can be efficiently decoded using the sum-product algorithm [6]. Under the channel condition assumed in [6] with N_R number of receive antennas, it was shown that the maximum achievable diversity order is $N_T \times N_R$.

For very high data rate transmissions, MIMO systems will have to operate in much larger bandwidths, resulting in intersymbol interference (ISI). Single-carrier MIMO with iterative joint equalization and decoding techniques is fast becoming an attractive scheme for realizing STC in frequency-selective channels [7], [8]. An optimum MIMO equalizer can suppress the ISI so that the output signal of the equalizer is ISI free. In fact, additional performance improvement can be obtained by taking advantage of the availability of multipath diversity inherent within these channels. Hence the maximum achievable diversity order for such a MIMO configuration is equals to $N_T \times L \times N_R$, where L is the number of paths [9].

In the past, most of the research efforts on STC have been focusing on the single-user point-to-point transmission scenario. It was only recently that attention has shifted to multiuser MIMO channels [10], [11]. Unfortunately, the performance of these receivers were studied assuming a flat fading channel. Thus, the additional burden of ameliorating the ISI was not considered. Hence in this paper, we will go one step further and consider the presence of both the multiple access interference (MAI) as well as ISI. Our objective is to propose a multiple access system that is capable of achieving the maximum diversity order as given by $N_T \times L \times N_R$. Specifically, we will create a signal processing platform that will allow the ST-WNRA codes to achieve the maximum diversity order over a frequency-selective Rayleigh fading MIMO channel in a multiuser environment, where each user equipped with N_T number of antennas attempts to communicate with a central base station having N_R number of antennas. In order to suppress the ISI and MAI, a turbo equalization technique based on the minimum mean square-error filtering with soft interference cancellation (SC-MMSE) is employed [12], [13]. More explicitly, the estimated MAI and ISI are first cancelled from the desired signal. Then based on an MMSE criterion, the multipath diversity that is available from the received signal will be fully exploited by transforming the frequency-selective faded desired signal to a vector of flat-faded signals. The symbols transmitted from all the antennas of each user during the same signalling interval will be detected jointly by the SC-MMSE detector, a technique which we have termed as joint-over antenna detection. We will show that by using this detection technique in conjunction with the ST-WNRA codes, the overall proposed system is capable of achieving the maximum diversity gain from the multiple antennas as well as from the multipath components, regardless of the number of users, and hence attaining an excellent bit error rate (BER) performance with a reasonable spectral efficiency at a low complexity cost.

II. System Model

We consider the uplink of a single cell synchronous K-user MIMO channel, as shown in Fig. 1. The ST-WNRA encoder of the $k$the user is shown in Fig. 2. The encoding and decoding of the ST-WNRA codes are performed on a frame-by-frame basis, where each frame consists of N number of uncoded information symbols. Basically, the encoding algorithm is similar to that given in [6] except that in our system, an inner interleaver is inserted after the accumulator, which can aid in improving the BER performance in frequency-selective channels. We can expressed the kth user's ST-WNRA codeword as a $N_T \times rN$ matrix $\mathbf{C}_k$ as [6]

$$\mathbf{C}_k = \begin{bmatrix} c_{k,1}(1) & \dots & c_{k,1}(rN) \\ \vdots & \ddots & \vdots \\ c_{k,N_T}(1) & \dots & c_{k,N_T}(rN) \end{bmatrix}, \quad (1)$$

where each row is assigned to a distinct transmit antenna. Independent ST-WNRA codewords will be transmitted by all K users at the same time and frequency without spreading. Provided that each repeated symbol corresponding to the same information symbol is

0-7803-8887-9/05/$20.00 (c)2005 IEEE

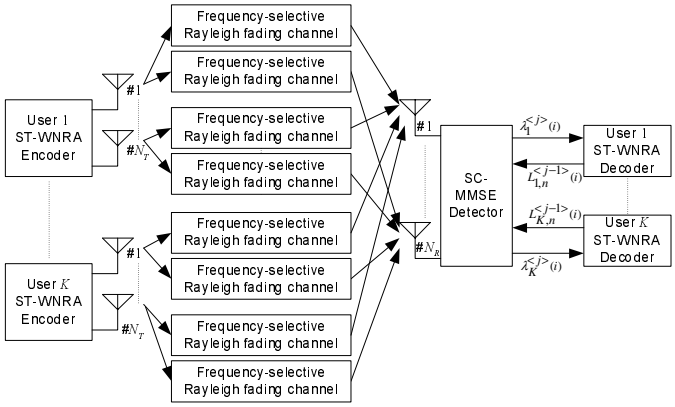

Fig. 1. ST-WNRA coded mulituser MIMO system model.

Fig. 2. The kth user's ST-WNRA encoder.

multiplied by a different weight as highlighted previously, the ST-WNRA codeword $\mathbf{C}_k$ will have a rank equivalent to $\min(r, N_T)$ in flat fading channels and a rate as given by N_T/r, as shown in [6].

A quasi-static L-path frequency-selective Rayleigh fading channel exists between each transmit-receive antenna pair. The lth complex path gain between the kth user's nth transmit antenna and the mth received antenna is denoted by $h_{k,n}^{(m)}(l)$ and these path gains are modelled as samples of independent zero mean complex Gaussian random variables. The equivalent vector representation of the received signals at the ith signaling interval can be written as

$$\mathbf{r}(i) \equiv \left[r^{(1)}(i)\dots r^{(N_R)}(i)\right]^T = \sum_{l=0}^{L-1}\mathbf{H}(l)\mathbf{c}(i-l)+\mathbf{v}(i), \quad (2)$$

where

$$\begin{aligned}\mathbf{H}(l) &= [\mathbf{H}_1(l)\dots\mathbf{H}_K(l)]\,;\mathbf{H}_k(l) = \left[\mathbf{h}_k^{(1)}(l)\dots\mathbf{h}_k^{(N_R)}(l)\right]^T\\ \mathbf{h}_k^{(m)}(l) &= \left[h_{k,1}^{(m)}(l)\dots h_{k,N_T}^{(m)}(l)\right]^T \end{aligned} \quad (3)$$

and

$$\mathbf{c}(i) = [\mathbf{c}_1(i)\dots\mathbf{c}_K(i)]^T\,;\mathbf{c}_k(i) = [c_{k,1}(i)\dots c_{k,N_T}(i)]\,. \quad (4)$$

The vector $\mathbf{v}(i)$ is the additive white Gaussian noise (AWGN). Temporal sampling is then performed to capture the multipath signals corresponding to the ith signalling interval for diversity combining, which yields the following space-time received signal vector

$$\mathbf{y}(i) \equiv \left[\mathbf{r}^T(i+L-1)\dots\mathbf{r}^T(i)\right]^T = \mathbf{H}\mathbf{b}(i)+\mathbf{n}(i), \quad (5)$$

where

$$\mathbf{H} = \begin{bmatrix} \mathbf{H}(0) & \dots & \mathbf{H}(L-1) & \dots & \mathbf{0} \\ \vdots & \ddots & \vdots & \ddots & \vdots \\ \mathbf{0} & \dots & \mathbf{H}(0) & \dots & \mathbf{H}(L-1) \end{bmatrix}, \quad (6)$$

$$\mathbf{b}(i) = \left[\mathbf{c}^T(i+L-1)\dots\mathbf{c}^T(i)\dots\mathbf{c}^T(i-L+1)\right]^T \quad (7)$$

and $\mathbf{n}(i) = \left[\mathbf{v}^T(i+L-1)\dots\mathbf{v}^T(i)\right]^T$. Note that if $L=1$ and $K=1$, full antenna diversity of order $N_T \times N_R$ can be obtained from the above signal using just the ST-WNRA decoder [6].

III. Turbo Equalization with ST-WNRA Codes

The iterative joint equalization and decoding receiver structure of the ST-WNRA codes is shown in Fig. 1. Basically, it consists of an SC-MMSE detector, followed by K parallel ST-WNRA decoders.

A. SC-MMSE Detector

The general structure of the SC-MMSE detector follows our work in [12]. Let us assumed that the SC-MMSE detector is current detecting the kth user's transmitted BPSK symbols during the ith transmission period, i.e., $c_k(i)$. At the jth iteration, the extrinsic LLR information of the coded BPSK symbols provided by the K ST-WNRA decoders from the previous iteration can be expressed as

$$L_{k,n}^{<j-1>}(i) = \log\frac{P\left[c_{k,n}(i)=+1\right]}{P\left[c_{k,n}(i)=-1\right]}, \quad (8)$$

where $L_{k,n}^{<0>}(i) = 0\,\forall\, k,n,i$. Based on the extrinsic LLR information given in Eq. (8), the SC-MMSE detector first forms soft estimates of the transmitted BPSK symbols of all the users as follows

$$\tilde{c}_{t,n}^{<j>}(i+l) = \begin{cases} \tanh\left\{\frac{L_{t,n}^{<j-1>}(i+l)}{2}\right\} & \text{for } t\neq k \text{ or } l\neq 0 \\ 0 & \text{for } t=k \text{ and } l=0. \end{cases} \quad (9)$$

Using these soft estimates, the interfering users' transmitted signals as well as the desired user's own ISI are then estimated and suppressed from the received signal according to

$$\tilde{\mathbf{y}}_k^{<j>}(i) = \mathbf{y}(i) - \mathbf{H}\tilde{\mathbf{b}}_k^{<j>}(i), \quad (10)$$

where $\tilde{\mathbf{b}}^{<j>}(i)$ is similar to that given in Eq. (7) except that the transmitted BPSK symbols are now replaced by the estimated symbols from Eq. (9). An MMSE filter is then invoked, in order to suppress the residual interferences in $\tilde{\mathbf{y}}_k^{<j>}(i)$. More explicitly, the filter weighting matrix $\mathbf{w}_k^{<j>}(i)$ is derived according to the following minimization criterion

$$\mathbf{w}_k^{<j>}(i) = \arg\min_{\mathbf{w}_k^{<j>}(i)} E\left\{\left[\mathbf{w}_k^{<j>^H}(i)\tilde{\mathbf{y}}_k^{<j>}(i) - \mathbf{A}_k\mathbf{c}_k^T(i)\right]^2\right\}, \quad (11)$$

where the matrix $\mathbf{A}_k = \left[\mathbf{H}_k^T(L-1)\dots\mathbf{H}_k^T(0)\right]^T$ with $\mathbf{H}_k(l)$ and $\mathbf{c}_k(i)$ given in Eq. (3) and Eq. (4), respectively. By observing the term $\mathbf{A}_k\mathbf{c}_k^T(i)$ in Eq. (11), it is clear that the objective of the MMSE filter in this case is to transform $\tilde{\mathbf{y}}_k^{<j>}(i)$ into a vector consisting of LN_R number of flat-faded desired signals that are free from any impairments, which is a major difference from those techniques shown in [13]. By doing this, not only is the transmit diversity of the ST-WNRA codes guaranteed, but also we can obtain additional diversity gain from the multipaths. Hence the maximum achievable diversity gain is in the order of $N_T \times L \times N_R$. It can be shown that the weighting matrix $\mathbf{w}_k^{<j>}(i)$ that satisfies Eq. (11) is given by [12]

$$\mathbf{w}_k^{<j>}(i) = \left[\mathbf{H}\mathbf{V}_k^{<j>}(i)\mathbf{H}^H + \sigma^2\mathbf{I}\right]^{-1}\mathbf{A}_k\mathbf{A}_k^H, \quad (12)$$

where

$$\begin{aligned}\mathbf{V}_k^{<j>}(i) &= \text{diag}\left\{1-\left[\tilde{c}_{1,1}^{<j>}(i+L-1)\right]^2,\dots,\right.\\ &\qquad \left. 1-\left[\tilde{c}_{K,N_T}^{<j>}(i-L+1)\right]^2\right\}. \end{aligned} \quad (13)$$

Hence the instantaneous MMSE estimate of the kth user's signal during the ith transmission period, denoted as $\mathbf{z}_k^{<j>}(i)$, is given by

$$\mathbf{z}_k^{<j>}(i) = \mathbf{w}_k^{<j>^H}(i)\tilde{\mathbf{y}}_k^{<j>}(i), \quad (14)$$

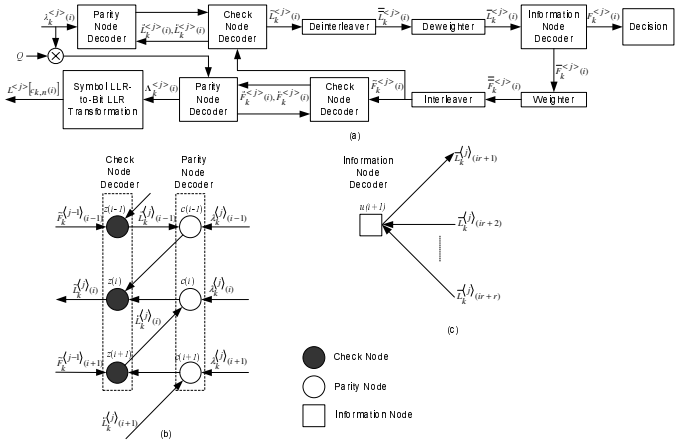

Fig. 3. (a) The kth user's ST-WNRA decoder. (b) Factor graph representation of the accumulator. (c) Factor graph representation of the repeater.

where $\mathbf{z}_k^{<j>}(i)$ can be modelled as a Gaussian process [12] having a mean $\mathbf{\Omega}_k^{<j>}(i)\mathbf{c}_k^T(i)$ and a covariance matrix $\mathbf{\Theta}_k^{<j>}(i)$. We can then calculate the extrinsic LLR vector of the transmitted coded GF(2^q) symbols $\hat{\lambda}_k^{<j>}(i) \equiv \left[\hat{\lambda}_k^{<j>}(i,0)\ldots\hat{\lambda}_k^{<j>}(i,2^q-1)\right]$, where the index (i,n) denotes the nth element in the LLR vector for the ith coded GF(2^q) symbol and $\hat{\lambda}_k^{<j>}(i,n)$ is given by

$$\hat{\lambda}_k^{<j>}(i,n) = \log\frac{P\left(c_k(i)=C_n\right)}{P\left(c_k(i)=C_0\right)} \text{ for } n=0,\ldots,2^q-1 \quad (15)$$

and

$$P\left(c_k(i)=C_n\right) = \exp\left\{-\left[\mathbf{z}_k^{<j>}(i)-\mathbf{\Omega}_k^{<j>}(i)\bar{\mathbf{c}}_n\right]^H \mathbf{\Theta}_k^{-1}(i)\left[\mathbf{z}_k^{<j>}(i)-\mathbf{\Omega}_k^{<j>}(i)\bar{\mathbf{c}}_n\right]\right\},$$

where $\mathbf{\Theta}_k^{<j>}(i) = \mathbf{\Omega}_k^{<j>}(i)\left\{\mathbf{A}_k^H - \mathbf{\Omega}_k^{<j>^H}(i)\right\}$, $\mathbf{\Omega}_k^{<j>}(i) = \mathbf{w}_k^{<j>^H}(i)\mathbf{A}_k$ and $\bar{\mathbf{c}}_n = [c_n(1)\ldots c_n(N_T)]^T$ is a BPSK representation of C_n, which follows the same mapping rule as employed by the transmitter. The coded GF(2^q) symbol LLR vector of each user is calculated for the entire frame, which is then appropriately deinterleaved according to the inner interleaving function before passing to the corresponding user's ST-WNRA decoder as $\lambda_k^{<j>}(i), i=1,\ldots,rN$, as shown in Fig. 1.

B. ST-WNRA Decoder

The structure of the kth user's ST-WNRA decoder is shown in Fig. 3(a), where the ST-WNRA codes can be efficiently decoded using the so-called message-passing algorithm, or more specifically the sum-product algorithm, based on the factor graphs as shown in Figs. 3(b) and 3(c). An excellent description of the sum-product algorithm of the accumulator was given in [15], which was based on a serial updating schedule as adopted in this paper. Hence in this contribution, we will only briefly highlight the flow of the algorithm. In keeping with the terminology used in a message-passing algorithm, we shall refer to these vectors as messages in our following discourse.

1) Messages from the Check Nodes to the Deinterleaver: The input to the kth user ST-WNRA decoder are the *a priori* LLR vectors of the coded GF(2^q) symbols corresponding to that user, as given in Eq. (15). The output messages from the check node decoder $\tilde{L}_k^{<j>}(i)$, as shown in Fig. 3(b), are computed according to

$$\tilde{L}_k^{<j>}(i) = \left[\lambda_{k,i}^{<j>}(i-1) + \overrightarrow{L}_k^{<j>}(i-1)\right] \odot \left[\lambda_k^{<j>}(i) + \overleftarrow{L}_k^{<j>}(i)\right], \quad (16)$$

where $\odot$ refers to a check operation, and the nth element in $\tilde{L}_k^{<j>}(i)$ is calculated according to [6]

$$[\alpha\odot\beta]_n = \log\frac{\sum_{\gamma\in\{C_0\ldots C_{2^q-1}\}}\exp\left(\alpha(\gamma)+\beta(\gamma\oplus n)\right)}{\sum_{\gamma\in\{C_0\ldots C_{2^q-1}\}}\exp\left(\alpha(\gamma)+\beta(\gamma)\right)}. \quad (17)$$

where $[\alpha\odot\beta]_n$ refers to the nth element of the vector denoted by $(\alpha\odot\beta)$ with $\alpha(\gamma)$ being the γth element in α. When $i=1$, $\lambda_{k,i}^{<j>}(0)$ and $\overrightarrow{L}_k^{<j>}(0)$ in Eq. (16) are designated as zero vectors. The messages $\overrightarrow{L}_k^{<j>}(i)$ and $\overleftarrow{L}_k^{<j>}(i)$ in Eq. (16), are calculated according to

$$\overrightarrow{L}_k^{<j>}(i) = \tilde{F}_k^{<j-1>}(i) \odot \left[\lambda_k^{<j>}(i-1) + \overrightarrow{L}_k^{<j>}(i-1)\right], \quad (18)$$

$$\overleftarrow{L}_k^{<j>}(i) = \tilde{F}_k^{<j-1>}(i+1) \odot \left[\lambda_k^{<j>}(i+1) + \overleftarrow{L}_k^{(j)}(i+1)\right], \quad (19)$$

where $\tilde{F}_k^{<j-1>}(i)$ are the messages delivered by the information nodes, after the outer interleaver, during the previous iteration. At the first iteration, $\tilde{F}_k^{<0>}(i)$ is a zero vector for $i=1,\ldots,rN$. Also, $\overrightarrow{L}_k^{<j>}(1) = \tilde{F}_k^{<j>}(1)$ and $\overleftarrow{L}_k^{<j>}(rN)$ is a zero vector in Eq. (18) and Eq. (19), respectively. The output messages $\tilde{L}_k^{<j>}(i), i=1,\ldots,rN$ are then deinterleaved accordingly and fed to the deweighter, as denoted by $\bar{\tilde{L}}_k^{<j>}(i)$ in Fig. 3(a).

2) De-weighter: The de-weighter, shown in Fig. 3(a), simply performs a cyclic shift of the elements in the input message $\bar{\tilde{L}}_k^{<j>}(i)$ according to the weighting value $\beta(i)$, except for the element $\bar{\tilde{L}}_k^{<j>}(i,0)$, in order to produce the message $\bar{L}_k^{<j>}(i)$ [6]. The de-weighted messages $\bar{L}_k^{<j>}(i), i=1,\ldots,rN$ are then fed to the information nodes.

3) Messages and Decisions from the Information Nodes: The information node corresponding to the $(i+1)$th information symbol is shown in Fig. 3(c). If the jth iteration is not the last iteration, then the output messages from the information nodes $\bar{F}_k^{<j>}(i)$ are calculated according to

$$\bar{F}_k^{<j>}(ir+x) = \sum_{y=1,y\neq x}^{r}\bar{L}_k^{<j>}(ir+y) \;\; i=0,\ldots,(N-1), \quad (20)$$

where $x=1,\ldots,r$. Otherwise, if the jth iteration is the last iteration, a decision on the $(i+1)$th uncoded information symbol is made based on the highest value LLR element in $F_k^{<j>}(i+1)$, where

$$F_k^{<j>}(i+1) = \sum_{y=1}^{r}\bar{L}_k^{<j>}(ir+y) \;\; i=0,\ldots,(N-1). \quad (21)$$

4) Messages to the SC-MMSE Detector: Following the computation of the message $\bar{F}_k^{<j>}(i)$ in Eq. (20), the elements in the message are again cyclic shifted, but in the reverse direction, by the weighter and interleaved to obtain $\tilde{F}_k^{<j>}(i)$. The extrinsic information from the kth user's ST-WNRA decoder to the SC-MMSE detector $\Lambda_k^{<j>}(i)$ are then derived according to

$$\Lambda_k^{<j>}(i) = \left[Q\times\lambda_k^{<j>}(i)\right] + \overleftarrow{F}_k^{<j>}(i) + \overrightarrow{F}_k^{<j>}(i), \quad (22)$$

where

$$\overrightarrow{F}_k^{<j>}(i) = \tilde{F}_k^{<j>}(i) \odot \left[\lambda_k^{<j>}(i-1) + \overrightarrow{F}_k^{<j>}(i-1)\right], \quad (23)$$

$$\overleftarrow{F}_k^{<j>}(i) = \tilde{F}_k^{<j>}(i+1) \odot \left[\lambda_k^{<j>}(i+1) + \overleftarrow{F}_k^{(j)}(i+1)\right]. \quad (24)$$

Following [10], a scaling factor Q is also introduced in Eq. (22) to enhance the iterative processing performance. However, notice that the scaled input extrinsic information $Q \times \lambda_k^{<j>}(i)$ is added to the output extrinsic information $\Lambda_k^{<j>}(i)$, instead of subtracting from it as found in [10]. This is due to the fact that the original input extrinsic information was omitted in the feedback path leading to the derivation of the corresponding output extrinsic information, as we can deduced from Eq. (20).

5) Symbol-to-bit LLR Transformation: The extrinsic information $\Lambda_k^{<j>}(i)$ provided by the parity bit decoder represents the LLR of the coded GF(2^q) symbols. Hence a symbol LLR-to-binary LLR transformation needs to be carried out, in order to produce the LLR of each coded BPSK symbol $L_{k,n}^{<j>}(i), n = 1, \ldots, N_T$ before the information can be used by the SC-MMSE detector, as defined by Eq. (9). The transformation is given by

$$L_{k,n}^{<j>}(i) = \log \frac{\sum_{d|c_{k,n}(i)=+1} P\{d = [c_{k,1}(i) \ldots c_{k,N_T}(i)]\}}{\sum_{d|c_{k,n}(i)=-1} P\{d = [c_{k,1}(i) \ldots c_{k,N_T}(i)]\}} \tag{25}$$

for $n = 1, \ldots, N_T$ and $P(d) = \exp\left[\Lambda_k^{<j>}(i,d)\right]$ with $d \in \{C_0, \ldots, C_{2^q-1}\}$ being the elements in GF(2^q).

C. Complexity

The complexity in the SC-MMSE detector is dominated by the matrix inversion of Eq. (12), which is in the order of $O\{L^3 N_R^3\}$ per coded GF(2^q) symbol per user per iteration. This complexity can be reduced by invoking the frequency-domain equalization techniques [16] as opposed to time-domain equalization methods adopted in this paper. The effective utilization of these techniques in conjunction with ST-WNRA codes will be left for future work.

Alternatively, it is also possible to iterate the information within the ST-WNRA decoder for several times, in order to improve its reliability before releasing the information to the SC-MMSE detector. This option may reduce the number of times required in performing the matrix inversion at the SC-MMSE detector and hence reduced the system complexity. Such approach has been proposed before, for example in [17] for LDPC codes.

In the context of the ST-WNRA decoder, it was shown in [15] that the sum-product algorithm for the accumulator requires about $1/6$ less operations per information bit as compared to that using the Bahl-Cocke-Jelinek-Raviv (BCJR) algorithm with binary code symbols. The same comparison analogy can also be applied to space-time trellis codes, which also uses the BCJR MAP decoding algorithm.

IV. Simulation Results

In this section, we investigate the performance of our proposed system using both GF(4) and GF(8) ST-WNRA codes having $N_T = 2$ and $N_T = 3$ transmit antennas, respectively. In our simulations, the uncoded frame length N is kept at 180 for GF(4) codes and 120 for GF(8) codes such that the number of information bits in a frame is kept the same for both codes. The number of repetitions r for both codes is maintained at 3. Hence for GF(4) ST-WNRA codes, the achievable rate is $2/3$ while full rate is achieved for GF(8) ST-WNRA codes. We also define E_b as the average information bit energy of each user's signal received by one antenna element and that all the users transmit with the same average power. Since we have assumed a quasi-static channel, the time diversity inherent in the ST-WNRA codes, which can significantly improve the performance of the codes in non quasi-static channels as shown in [6], is not exploited here. Also, unless specified, the channels are assumed to be independent among the transmit-receive antenna pairs.

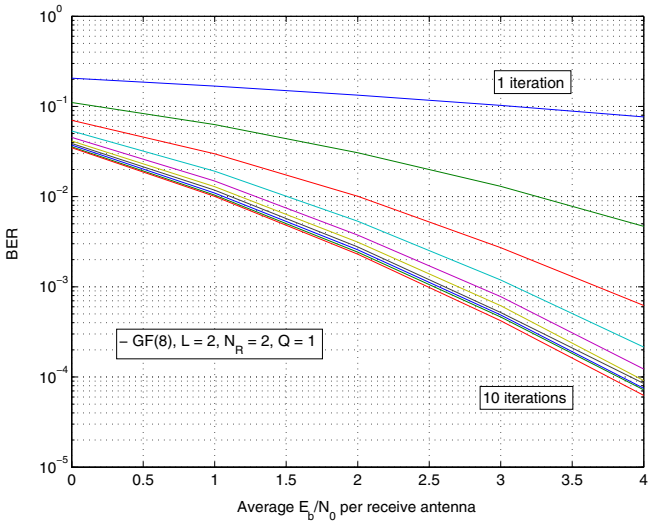

Fig. 4. BER performance versus the number of iterations for $L = 2, N_R = 2$ and $Q = 1$.

Recall that the complexity of our proposed iterative system, in particularly the SC-MMSE detector, increases with increased number of multipath components and receive antennas. One way of reducing the complexity of the system is by reducing the number of iterations before making the ultimate decision on the information data, while sacrificing some performance loss. The convergence behaviour of our system is illustrated in Fig. 4 for the case of one user with $L = 2, N_R = 2$ and $Q = 1$ for GF(8) codes. As we can see, the difference in performance beyond the 6th iteration is insignificant. Moreover, it can be easily verified that the slope of the performance curves beyond five iterations corresponds to a diversity order of 12, which is as we have expected. Similar observations were also exhibited for GF(4) codes (not shown here). Due to the diminishing returns in the performance as well as the high complexity involved in the iterative process, only 6 iterations will be performed for our subsequent simulations.

In multiuser cases, the BER was found to be enhanced if the Q values are set to 1 and 0.5 for GF(4) and GF(8) codes, respectively. Fig. 5 shows the performance of the proposed system with multiple users for GF(4) and GF(8) ST-WNRA codes. For comparison, the single-user BER under the same system conditions are also shown. As we can see from the figure, with $K = 2$ and $N_R = 2$, the BER degrades by about 0.5dB and 1dB for GF(4) and GF(8) codes, respectively, relative to the single-user bound. On the other hand, when $N_R = 3$, the BER performance with two users approaches the single-user bound. This is because the additional antennas are able to preserve the degrees-of-freedom of the SC-MMSE detector that can be used to cancel the other users' signals [12]. We can also observe that the BER degrades by about 0.25 dB with three users. More importantly, however, we observed that the slope of the curves with multiple users is the same as that of the corresponding single-user case. This implies that the achievable diversity order is maintained regardless of the number of users present. We can also see that the slope of curves corresponding to GF(4) codes with three receive antennas is the same as that with GF(8) codes having two receive antennas. This conforms to our proposition that the achievable diversity order of our system is indeed given by $N_T \times L \times N_R$.

In the event of insufficient antenna spacing, the assumption of a

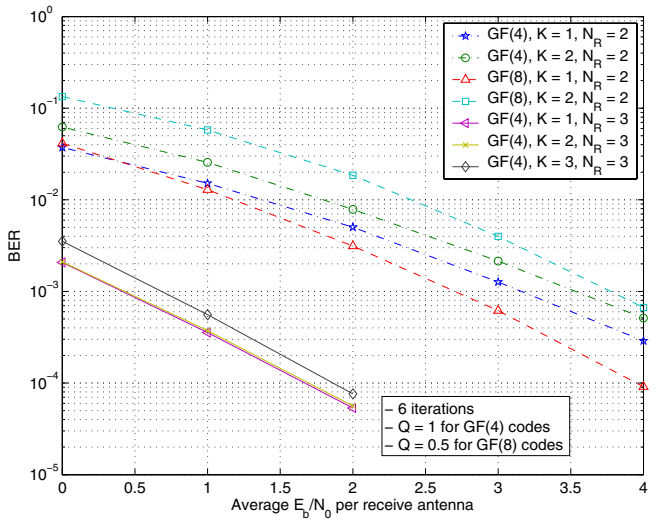

Fig. 5. Performance comparison of GF(4) and GF(8) ST-WNRA codes with various number of users and receive antennas, and $L = 2$.

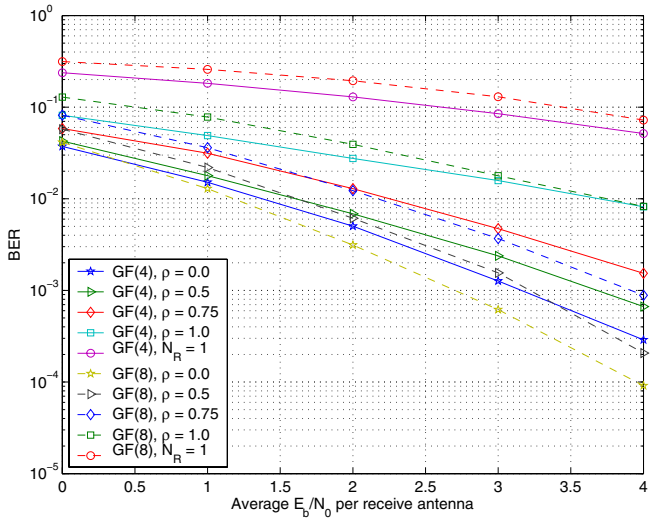

Fig. 6. BER performance on correlated frequency-selective fading channels with $L = 2, N_R = 2$ and $Q = 1$.

spatially independent channel is no longer true. It has been shown in [18] that the presence of spatial fading correlation can degrade the performance of STC. Fig. 6 shows the performance of GF(4) and GF(8) codes in correlated Rayleigh fading channel with $L = 2$ and $N_R = 2$ and a single user. The correlation coefficient ρ between the two receive antennas are chosen to be 0, 0.5, 0.75 and 1.0. The BER performances of these codes with $L = 2$ and $N_R = 1$ are also shown in the figures for comparison sake. As we can see, when $\rho = 0.5$, there is only a slight degradation in the performance as compared to the uncorrelated case, i.e., $\rho = 0$. However, as the correlation between the receive antennas increases, the performance is degraded. In fact, when the receive antennas are fully correlated, i.e., $\rho = 1$, the benefit of having the receive antenna diversity no longer exists. In this case, the achievable diversity gain is only due to the ST-WNRA codes and the multipath components. As we can see from the figures, the slopes of GF(4) and GF(8) codes for $\rho = 1$ corresponds to a diversity order of 4 and 6, respectively, which is the same as that for $L = 2$ and $N_R = 1$, but are shifted by 3 dB due to the additional antenna gain.

V. Conclusion

We studied the performance of the ST-WNRA codes over a frequency-selective Rayleigh fading MIMO channel in a multiuser environment. The SC-MMSE detector was designed so that the diversity that can be gleaned from the multiple antennas as well as from the multipath components can be fully exploited. It was demonstrated that the proposed system is capable of attaining the diversity gain obtained from the transmit and receive antennas as well as the multipath components and that the same achievable diversity order is maintained in a multiuser environment.

References

[1] I. E. Telatar, "Capacity of multi-antenna gaussian channels," *Eur. Trans. Telecommun.*, vol. 10, no. 6, pp. 585–595, Nov. 1999.

[2] G. J. Foschini and M. J. Gans, "On limits of wireless communications in a fading environment when using multiple antennas," *Wireless Pers. Commun.*, vol. 6, pp. 311–335, Mar. 1998.

[3] V. Tarokh, N. Seshadri and A. R. Calderbank, "Space-time codes for high data rate wireless communication: Performance criterion and code construction," *IEEE Trans. Inform. Theory*, vol. 44, pp. 744–765, Mar. 1998.

[4] S. M. Alamouti, "A simple transmitter diversity scheme for wireless communications," *IEEE J. Select. Areas Commun.*, vol. 16, pp. 1451–1458, Oct. 1998.

[5] G. J. Foschini, "Layered space-time architecture for wireless communication in a fading environment when using multi-element antennas," *Bell Labs. Tech. J.*, vol. 1, no. 2, pp. 41–59, 1996.

[6] J.-E. Oh and K. Yang, "Space-time codes with full antenna diversity using weighted nonbinary repeat-accumulate codes," *IEEE Trans. Commun.*, vol. 51, pp. 1773–1778, Nov. 2003.

[7] G. Bauch and N. Al-Dhahir, "Reduced-complexity space-time turbo-equalization for frequency-selective MIMO channels," *IEEE Trans. Wireless Commun.*, vol. 1, pp. 819–828, Oct. 2002.

[8] X. Wautelet, A. Dejonghe and L. Vandendorpe, "MMSE-based fractional turbo receiver for space-time BICM over frequency-selective MIMO fading channels," *IEEE Trans. Signal Processing*, vol. 52, pp. 1804–1809, Jun. 2004.

[9] M. Qin and R. S. Blum, "Properties of space-time codes for frequency-selective channels," *IEEE Trans. Signal Processing*, vol. 52, pp. 694–702, Mar. 2004.

[10] B. Lu and X. Wang, "Iterative receivers for multiuser space-time coding systems," *IEEE J. Select. Areas Commun.*, vol. 18, pp. 2322–2335, Nov. 2000.

[11] B. K. Ng and E. S. Sousa, "On bandwidth-efficient multiuser-space-time signal design and detection," *IEEE J. Select. Areas Commun.*, vol. 20, pp. 320–329, Feb. 2002.

[12] N. Veselinovic and T. Matsumoto, "Space-time coded turbo equalization and multiuser detection - Asymptotic performance analysis in the presence of unknown interference," *Asilomar Conf. Signals, Syst., Comput.*, submitted for publication.

[13] T. Abe and T. Matsumoto, "Space-time turbo equalization in frequency-selective MIMO channels," *IEEE Trans. Veh. Technol.*, vol. 52, pp. 469–475, May 2003.

[14] D. Tujkovic, M. Juntti and M. Latva-aho, "Space-frequency-time turbo coded modulation," *IEEE Commun. Lett.*, vol. 5, pp. 480–482, Dec. 2001.

[15] J. Li, K. R. Narayanan and C. N. Georghiades, "Product accumulate codes: A class of codes with near-capacity performance and low decoding complexity," *IEEE Trans. Inform. Theory*, vol. 50, pp. 31–46, Jan. 2004.

[16] M. S. Yee, M. Sandell and Y. Sun, "Comparison study of single-carrier and multi-carrier modulation using iterative based receiver for MIMO system", in *Proc. IEEE VTC*, Milan, Italy, May 2004.

[17] Heung-no Lee and V- Gulati, "Iterative equalization/decoding of LDPC code transmitted over MIMO fading ISI channels", in *Proc. IEEE Int. Symp. Personal, Indoor, and Mobile Radio Commun.*, Lisbon, Portugal, vol. 3, pp. 1330-1336, Sept. 2002.

[18] J. Wang, M. K. Simon, M. P. Fitz and K. Yao, "On the performance of space-time codes over spatially correlated Rayleigh fading channels," *IEEE Trans. Commun.*, vol. 52, pp. 877–881, Jun. 2004.